Research Article

Mathematical Methods in the Applied Sciences

Received 20 February 2013

Published online 25 June 2013 in Wiley Online Library

(wileyonlinelibrary.com) DOI: 10.1002/mma.2852
MOS subject classification: 76A05; 76M99; 65C30

An energetic variational approach to ion channel dynamics

YunKyong Hyon[a*†], Bob Eisenberg[b] and Chun Liu[c]

Communicated by Q. Wang

We introduce a mathematical model to study the transport of ions through ion channels. The system is derived in the framework of the energetic variational approach, taking into account the coupling between electrostatics, diffusion, and protein (ion channel) structure. The geometric constraints of the ion channel are introduced through a potential energy controlling the local maximum volume inside the ion channel. A diffusive interface (labeling) description is also employed to describe the geometric configuration of the channels. The surrounding bath and channel are smoothly connected with the antechamber region by this label function. A corresponding modified Poisson–Nernst–Planck channel system for ion channels is derived using the variational derivatives of the total energy functional. The functional consists of the entropic free energy for diffusion of the ions, the electrostatic potential energy, the repulsive potential energy for the excluded volume effect of the ion particles, and the potential energy for the geometric constraints of the ion channel. For the biological application of such a system, we consider channel recordings of voltage clamp to measure the current flowing through the ion channel. The results of one-dimensional numerical simulations are presented to demonstrate some signature effects of the channel, such as the current output produced by single-step and double-step voltage inputs. Copyright © 2013 John Wiley & Sons, Ltd.

Keywords: energetic variational approach; Poisson–Nernst–Planck equation; diffusive interface method; finite size effect; repulsive potential; ion channel; voltage clamp

1. Introduction

We introduced a mathematical model for the dynamics of ion transport through ion channels (protein pores) that takes into account excluded volume (finite size) effects of ion particles in [1–3] as well as electric and geometric configurations of the channels. The models for ionic fluids are natural extensions of the classical Poisson–Nernst–Planck (PNP) and Poisson–Boltzmann theories. The excluded volume effect (finite size effect or steric size effect) is included by adding a repulsive potential to the free energy functional. The resulting partial differential–integral system can be systematically derived with the energetic variational approach [1–4].

The free energy of the classical PNP system for diluted solutions includes only the entropic free energy and the electrostatic energy (see [5] and its references). In [2, 3], we studied a free energy including the entropy of ion particle diffusions, the electrostatic energy for interaction of ions with the environments and among themselves, together with a repulsive potential energy for the finite size effect of ions. This produced a modified Poisson–Nernst–Planck (MPNP) system. In [2, 3], we have shown that the MPNP system captures many signature phenomena of nondilute ionic fluids, such as charge inversion (layering) phenomena, which are an alternating accumulation of charges near a charged wall under the strong influence of a spatially varying electric force [2].

Proteins such as ion channels are involved with most activities of living cells, and control the ionic fluid flows between intracellular and extracellular regions of a cell. In this paper, we are interested in the dynamics of ionic fluids through such ion channels, which possess specific geometric and electric configurations [6–11]. An ion channel is made up of a specific type of protein, which forms a path for ions and has electrostatic properties that characterize the ion channel [12–16].

The geometric size (constraint) of a channel can be established by a potential energy that controls the local maximum volume inside the ion channel. We characterize the ion channel with a diffusive interface representation [17–22]. The diffusive interface method provides many important advantages in this mathematical modeling of ion channels. The resulting system does not need to have

[a] *Division of Mathematical Models, National Institute for Mathematical Sciences, Daejeon 305-811, Korea*
[b] *Department of Molecular Biophysics & Physiology Rush Medical Center, 1653 West Congress, Parkway, Chicago, IL 60612, USA*
[c] *Department of Mathematics, Pennsylvania State University, University Park, PA 16802, USA*
**Correspondence to: YunKyong Hyon, Division of Mathematical Models, National Institute for Mathematical Sciences, Daejeon 305-811, Korea.*
[†] *E-mail: hyon@nims.re.kr*

any additional boundary condition for the interface between the ion channel and the bath. The antechamber of the channel can be modeled without any geometric stiffness or singularity, which is also a benefit in numerical computations. The channel can have a mechanical property (the hardness/softness of the channel) with the coefficient of the potential energy that indicates its strength for the channel. In modeling of the ion channel, other key features are the electrical properties of the channel protein, which play a critical role in determining the electrostatic potential inside the channel. We model these properties by including extra permanent charges, movable or fixed (as in this paper), inside the channel. The details of this simple and effective approach can be found in [2, 3].

The total free energy is defined by the sum of the entropy, the electrostatic potential energy, the finite size energy for the ion particles, and the potential energy for the geometric constraints of the channel. The resulting mathematical system is then derived by the variational derivatives of the total energy with respect to the ion concentration, and automatically satisfies the dissipative energy law. This latter fact is one of the key advantages of the energetic variational approach. We denote the resulting system of integro-differential equations as the modified Poisson–Nernst–Planck channel (MPNP-C) systems. The energetic variational approach and the resulting systems can be in any dimension and are, in principle, suitable for any geometric environment.

As applications and validations of the MPNP-C, we consider a single channel recording of current produced by applying a variety of pulses as voltage inputs to the system. Such voltage protocols have been widely used to define channel properties for many years [23–25]. Single channel recording is the standard experimental protocol in thousands of papers studying ion channels [26]. Our numerical simulations are aimed at reproducing similar results in realistic experimental settings. For instance, in the numerical experiments, the input pulse used so extensively in voltage clamp experiments can be realized by the time dependent Dirichlet boundary conditions of the electrostatic potential. We will focus on a one-dimensional setting of the system in our numerical simulations. One dimensional settings have a special role because they allow an investigation of ranges of parameters and models that is valuable in the exploration ('reverse engineering') of biological systems. However, this can be easily extended to a high-dimensional situation, for instance, to a cylinder type ion channel.

This paper is organized as follows. Section 2 discusses the energetic variational approach and the basic form of the system. In Section 3, we review the free energy functionals and the derivations of both PNP and MPNP systems. In Section 4, we introduce the potential energy for the geometric configuration of an ion channel and derive the MPNP-C for the channel dynamics. Finally, the numerical results and discussions of the resulting mathematical system for single-step and the double-step pulses experiments are presented in Section 5.

2. Energetic variational approach and conservation laws

The energetic variational approach for complex fluids is based on two basic physical principles, the least action principle for the conservative (reversible) part of the system, and Onsager's maximum dissipation principle for the dissipative (irreversible) part of the system [2–4].

All the physics and the constraints of the problem are included in the choice of the free energy and dissipation functionals. Once they are determined, together with the kinematic transport properties of the dynamic variables, the system is uniquely determined by the variational procedure. An example of the energetic variational approach is the incompressible Navier–Stokes equations for Newtonian fluids [1–4]. In this case, the least action principle gives the Euler equation, which is the conservative part of the Navier–Stokes equations, and the maximum dissipation principle gives the Stokes equations, which is the dissipative part of the system. The advantages of this approach are the flexibility of easily incorporating with different physics (even from different scales) and the fact that the resulting self-consistent systems automatically satisfy the second law of thermodynamics.

For the problem of ion transport, the ionic concentrations, c_i for different ions, will satisfy the following conservation laws:

$$\frac{\partial c_i}{\partial t} + \nabla \cdot \vec{J}_i = 0 \quad \text{for } i = 1, \cdots, N. \tag{1.1}$$

Here, $\vec{J}_i$ is the ionic flux of the ith ion species, and N is the number of types of ions. The electrostatic potential ϕ satisfies the Poisson equation,

$$-\nabla \cdot (\varepsilon \nabla \phi) = \rho_0 + \sum_{i=1}^{N} z_i q c_i \tag{1.2}$$

where ε is the dielectric constant, ρ_0 the permanent charge density in the system, z_i is the valence of ith ion species, and q is the unit charge. Together, these equations are the form of Maxwell's equations appropriate when magnetic forces are insignificant [27].

Notice that it is not difficult to treat the movable permanent charge densities. One way is to introduce another dynamic transport equation for the concentration and also an additional energy functional to confine the charges in the channel. In fact, one can identify a portion of the electrostatic characteristics of the channel protein by these movable permanent charges in the system. Such a motion of the permanent charge can also be related to the conformational changes of the proteins. The charges induced on the boundaries of the overall system by these conformational changes are called 'gating currents' in the physiological literature. The energetic variational approach computes such deformations/changes self-consistently as part of the solution of the mathematical model. Such interactions are a possible cause of the instability in the current observed as the spontaneous opening and closing of a channel.

The physics of different systems are reflected through the flux functions in (1.1). In most systems, the microscopic part is considered to be near electrostatic and thermal equilibrium. The system represents the combination of a deterministic gradient flow with

stochastic Brownian motions. Often, the distribution of velocities is a displaced Maxwellian [28–31]. This is also consistent with the linear response theory for near equilibrium (nearly Maxwellian) systems.

In Section 3, we first briefly discuss a derivation of classic PNP equations using the energetic variational approach [5] and then extend it to MPNP systems [1]. This will naturally lead to the channel system MPNP-C in Section 4.

3. Dynamics of ion transport: PNP and MPNP systems

3.1. Poisson–Nernst–Planck system

Starting with the total energy equation of the electrokinetic theory for charged ions, one can apply the energetic variational approach to obtain the transport equations of the PNP systems for ionic concentrations. The resulting transport equations are then coupled with the Poisson equation (1.2) of the electrostatic potential [1–3].

The total energy $E_{\mathrm{PNP}}^{\mathrm{total}}$ for the ion transport includes (i) the entropic free energy for the Brownian motion of ion particles and (ii) the electrostatic potential energy produced by the Coulomb interaction among ions. The explicit form of $E_{\mathrm{PNP}}^{\mathrm{total}}$ is given by

$$E_{\mathrm{PNP}}^{\mathrm{total}} = \int \left\{ \mathrm{k_B T} \sum_{i=1}^{N} c_i \log c_i + \frac{1}{2} \left(\rho_0 + \sum_{i=1}^{N} z_i q c_i \right) \phi \right\} \mathrm{d}\vec{x} \tag{2.1}$$

where $\mathrm{k_B}$ is the Boltzmann constant and T is the temperature. Then, the ionic flux resulting from the averaged force is $\vec{J}_i = -\frac{D_i}{k_B T} c_i \nabla \mu_i$ for $i = 1, \cdots, N$, where $\mu_i = \frac{\delta E_{\mathrm{PNP}}^{\mathrm{total}}}{\delta c_i}$ is the chemical potential for the ith ion species. D_i is the diffusion constant of ith ion species [1–3, 5].

Remark 3.1

The second term in the total energy (2.1) is equal to $\int \varepsilon \frac{|\nabla \phi|^2}{2} \mathrm{d}\vec{x}$ using the appropriate boundary condition for the electrostatic potential. It is exactly the electrostatic potential energy as in classical electric theories [32]. However, because in dynamical situations, it is the charge that is transported by the fields, the suitable variables in the variational procedure will be the ionic concentration.

Combining with (1.1), (1.2), we have the PNP equation as follows:

$$\frac{\partial c_i}{\partial t} = \nabla \cdot \left(D_i \left(\nabla c_i + \frac{z_i q}{\mathrm{k_B} T} c_i \nabla \phi \right) \right), \tag{2.2}$$

$$\nabla \cdot (\varepsilon \nabla \phi) = -\left(\rho_0 + \sum_{i=1}^{N} z_i q c_i \right). \tag{2.3}$$

The detailed derivation of the PNP system can be found in [2, 3]. The PNP system (2.2), (2.3) satisfies the following dissipative energy law:

$$\begin{aligned} &\frac{\mathrm{d}}{\mathrm{d}t} \int \left\{ \mathrm{k_B} T \sum_{i=1}^{N} c_i \log c_i + \frac{1}{2} \left(\rho_0 + \sum_{i=1}^{N} z_i q c_i \right) \phi \right\} \mathrm{d}\vec{x} \\ &= -\int \left\{ \sum_{i=1}^{N} \frac{D_i c_i}{\mathrm{k_B} T} \left| \mathrm{k_B T} \frac{\nabla c_i}{c_i} + z_i q \nabla \phi \right|^2 \right\} \mathrm{d}\vec{x}. \end{aligned} \tag{2.4}$$

The classical PNP system has also been used extensively in the study of the semiconductor devices [28, 29, 33].

3.2. Modified Poisson–Nernst–Planck system

For non-dilute ionic fluids, one needs to consider the finite size of ion particles. The potential energy for the excluded volumes of ion particles can be represented by a regularized repulsive interaction potential in [1–3]. As an approximation to the hard core repulsion, for convenience, we use a regularized repulsive potential generated by the repulsive part of the Lennard–Jones (LJ) potential. The energy of repulsion is the defined by

$$E_{\mathrm{LJ}}^{\mathrm{repulsion}} = \sum_{i=1}^{N} \sum_{j \geq i}^{N} \frac{1}{2} \int \int \Psi_{i,j}(|\vec{x} - \vec{y}|) c_i(\vec{x}, t) c_j(\vec{y}, t) \, \mathrm{d}\vec{x} \mathrm{d}\vec{y}. \tag{2.5}$$

The repulsive interaction potential is $\Psi_{i,j}(|\vec{x} - \vec{y}|) = \frac{\varepsilon_{i,j}(a_i + a_j)^{12}}{|\vec{x} - \vec{y}|^{12}}$ for ith and jth ions located at $\vec{x}$ and $\vec{y}$. The particle radii are a_i, a_j, respectively. $\varepsilon_{i,j}$ are energy constants. The total energy of the MPNP system is then defined by

$$E_{\mathrm{MPNP}}^{\mathrm{total}} = E_{\mathrm{PNP}}^{\mathrm{total}} + E_{\mathrm{LJ}}^{\mathrm{repulsion}}.$$

The MPNP system is derived by the same variational derivatives of $E^{\text{total}}_{\text{MPNP}}$ as those for PNP systems [1–3, 5].

$$\frac{\partial c_i}{\partial t} = \nabla \cdot \left[D_i \left\{ \nabla c_i + \frac{z_i q c_i}{k_B T} \nabla \phi + \frac{c_i}{k_B T} \nabla \psi_{r,i} \right\} \right], \quad \text{for } i = 1, \cdots, N, \tag{2.6}$$

$$\nabla \cdot (\varepsilon \nabla \phi) = -\left(\rho_0 + \sum_{i=1}^{N} z_i q c_i \right) \tag{2.7}$$

where

$$\psi_{r,i} = \frac{1}{2} \int \left\{ \sum_{j=1}^{N} \Psi_{i,j} c_j(\vec{y}, t) + \Psi_{i,i} c_i(\vec{y}, t) \right\} d\vec{y}.$$

Moreover, the MPNP system consisting of (2.6) and (2.7) satisfies the following dissipative energy law:

$$\begin{aligned} &\frac{d}{dt} \int \left\{ k_B T \sum_{i=1}^{N} c_i \log c_i + \frac{1}{2} \left(\rho_0 + \sum_{i=1}^{N} z_i q c_i \right) \phi + \sum_{\substack{i=1 \\ j \geq i}}^{N} \int \frac{\Psi_{i,j}(|\vec{x} - \vec{y}|)}{2} c_i(\vec{x}, t) c_j(\vec{y}, t) \, d\vec{y} \right\} d\vec{x} \\ &= -\int \left\{ \sum_{i=1}^{N} \frac{D_i c_i}{k_B T} \left| k_B T \frac{\nabla c_i}{c_i} + z_i q \nabla \phi + \nabla \psi_{r,i} \right|^2 \right\} d\vec{x}. \end{aligned} \tag{2.8}$$

4. Ion channel dynamics: MPNP-C system

For a specific ion channel, the shape and size of the pore (within the channel protein) will be treated as geometric constraints. In our modeling approach, we use the diffusive interface (labeling) method [21, 22], which describes the interfacial region between two regions (phases and states). The diffusive interface method provides a smooth antechamber region of the channel. Moreover, in this approach, the hardness/softness of the ion channel is established by the energy coefficient of the potential energy. Careful adjustment of the stiffness of the antechamber (and/or diameter) is needed to avoid numerical instability. We do not know yet if the sensitivity to stiffness is a property of our numerical procedures or whether it reflects the instability of ion channel currents always observed in experiments called 'single channel gating'.

Diffusive interface methods, and other Eulerian coordinate methods such as level set methods and finite volume methods, are widely used in the description of problems involving complicated shapes or vastly contrasting regions. These methods may prove to be particularly useful, even necessary, for dealing with the shapes of proteins in the sense of field theory approximation, including ion channels and enzymes. The details of these shapes are widely believed to be important determinants of most biological functions. The nature of Eulerian descriptions also make them easier to adapt to the energetic variational approach.

The natural label function (characteristic function) representing the channel and the bulk satisfies

$$\chi_{\text{label}} = \begin{cases} 0, & \text{for the channel,} \\ 1, & \text{for the bulk.} \end{cases} \tag{3.1}$$

The following diffusive interface function (phase function) χ will be the smooth approximation of the original label function χ_{label}:

$$\chi(\vec{x}) = \frac{1}{2} \left\{ \tanh \left(\frac{d(\vec{x})}{\sqrt{2}\eta} \right) + 1 \right\}, \tag{3.2}$$

where $d(\vec{x})$ is the distance function from the antechamber and η is related to the thickness (length) of the antechamber.

For the geometric constraint of the channel, we can define a potential energy using the local maximum volume of the channel.

$$E^{\text{channel}} = \int (1 - \chi^2)^2 \frac{A}{2} \left\{ \tanh \left(\frac{m(\vec{x}, t) - M(\vec{x})}{\eta_0} \right) + 1 \right\} d\vec{x}. \tag{3.3}$$

This energy functional reflects some mechanical properties of the channel. The coefficient A can be viewed as an overall stiffness coefficient and η_0 the local stiffness coefficient. The choices of these parameters provide certain extensibility (elasticity) of the channel. The larger the parameter A (and the smaller η_0), the harder (stiffer) the channel is. $M(\vec{x})$ is the local maximum volume of channel with unit length. For any given moment at time t, $m(\vec{x}, t)$ is the total instantaneous volume of ions at position $\vec{x}$ with the unit length. The explicit forms of $M(\vec{x})$ and $m(\vec{x}, t)$ are defined by

$$M(\vec{x}) = s R_{ch}^2(\vec{x}) \pi, \quad m(\vec{x}, t) = \sum_{i=1}^{N} \frac{4 a_i^3 \pi}{3} M(\vec{x}) c_i(\vec{x}, t) \tag{3.4}$$

where $R_{ch}(\vec{x})$ is the channel radius at position $\vec{x}$ and s is the unit length.

Remark 4.1

The geometric constraint of an ion channel is a key feature in the study of ion channels in cell membrane, especially, in applying the field theory to it. This is a realization of the physical configuration of an ion channel in terms of potential energy used in this form here, for the first time, as far as we know. Because the potential energy functional of the geometric constraint of the channel does not require any other additional boundary conditions in the energetic variational approach, we can extend the applicability of PNP type system of PDEs to more realistic situations of ion channel. However, additional numerical treatments may be needed in computations of the resulting system.

Moreover, the establishment of the geometric constraint can be used in higher dimensional space. In fact, the forms of $M(\vec{x})$ and $m(vx)$ already include higher dimensional aspect.

The use of the hyperbolic tangent function in the channel potential energy (3.3) provides specific constraints of the channel geometry with respect to current through the channel. When the instantaneous ion volume $m(\vec{x},t) < M(\vec{x})$, the ions flow freely through the channel without any constraint from the channel. The energy will penalize the situation when the instantaneous ion volume $m(\vec{x},t)$ exceeds the local maximum volume $M(\vec{x})$.

The variational derivative of (3.3) with respect to the ionic concentration c_i leads us to

$$\delta E^{\text{channel}} = \frac{A}{2}\int (1-\chi^2)^2 \operatorname{sech}^2\left(\frac{m(\vec{x},t)-M(\vec{x})}{\eta_0}\right)\left(\frac{4a_i^3\pi M(\vec{x})}{3\eta_0}\right)\delta c_i \,\mathrm{d}\vec{x}. \tag{3.5}$$

Finally, we have the MPNP-C system, for $i = 1, \cdots, N$,

$$\frac{\partial c_i}{\partial t} = \nabla\cdot\left[D_i\left\{\nabla c_i + \frac{z_i q c_i}{\mathrm{k_B}T}\nabla\phi + \frac{c_i}{k_B T}\nabla(\psi_{r,i}+\psi_{ch,i})\right\}\right], \tag{3.6}$$

$$\nabla\cdot(\varepsilon\nabla\phi) = -\left(\rho_0 + \sum_{i=1}^{N} z_i q c_i\right) \tag{3.7}$$

where

$$\psi_{ch,i} = \frac{A}{2}(1-\chi^2)^2\operatorname{sech}^2\left(\frac{m(\vec{x},t)-M(\vec{x})}{\eta_0}\right)\left(\frac{4a_i^3\pi M(\vec{x})}{3\eta_0}\right). \tag{3.8}$$

The MPNP system ((3.6), (3.7)) satisfies the following dissipative energy law:

$$\begin{aligned}\frac{\mathrm{d}}{\mathrm{d}t}\int\left\{\mathrm{k_B}T\sum_{i=1}^{N}c_i\log c_i + \frac{1}{2}\left(\rho_0+\sum_{i=1}^{N}z_i q c_i\right)\phi + \sum_{\substack{i=1\\ j\geq i}}^{N}\int\frac{\Psi_{i,j}(|\vec{x}-\vec{y}|)}{2}c_i(\vec{x},t)c_j(\vec{y},t)\,\mathrm{d}\vec{y}\right\}\mathrm{d}\vec{x}\\ = -\int\left\{\sum_{i=1}^{N}\frac{D_i c_i}{\mathrm{k_B}T}\left|\mathrm{k_B}T\frac{\nabla c_i}{c_i} + z_i q\nabla\phi + \nabla\psi_{r,i} + \nabla\psi_{ch,i}\right|^2\right\}\mathrm{d}\vec{x}.\end{aligned} \tag{3.9}$$

Remark 4.2

As we presented in previous sections, the resulting mathematical systems of PDEs can be systematically derived by the energy variational framework. The mathematical systems, PNP, MPNP, and MPNP-C satisfy the dissipative energy law (2.4), (2.8), and (3.9), respectively, which guarantees the stability of the system at the continuum level.

In the next section, we present the numerical results of the MPNP-C system (3.6), (3.7) with a biophysical application.

5. Numerical experiments

We consider a numerical 'voltage clamp' experiment of the ion channel for a verification of the MPNP-C system (3.6), (3.7). In the numerical experiment, we will focus on the one-dimensional models for the channel dynamics. This is mainly due to the limitation of the simulation capacity, although one-dimensional models will always have their role in the study of these complicated coupled systems, in particular in investigations of inverse problems. The voltage clamp experiment measures the charge and current flowing along the channel in response to a voltage that is forced (i.e., 'clamped') to follow a definite time course. The numerical computations are performed in one-dimensional space with the domain, $[-60, 60]$Å. The ion channel is located in $[-10, 10]$Å with its radius 3.5Å. The dielectric constant is 80 for the ionic solution in the bath and 8 in the channel with a taper as

$$\varepsilon(x) = \frac{b_1}{2}\left\{\tanh\left(\frac{d(x)}{\sqrt{2}\eta}\right)+1\right\} + b_2,$$

where $b_1 = 72$, $b_2 = 8$ for the dielectric constant in the bath and the channel. In all the computations, except those in Figure 3 (top row), the permanent charge is taken to be $\rho_0 = -0.227$. The ionic electrolyte solution is chosen as the mixture of Na^+ and Cl^- ions

with their ion radius $a_{Na} = 1.801$Å and $a_{Cl} = 1.02$Å, respectively. The energy coefficients $\varepsilon_{i,j} = 0.05$ for $i, j = 1, 2$, $A = 1.5$, and the temperature is $T = 281.5$K. The schematic diagram of the domain with the profile of the phase function χ is presented in Figure 1.

The single-step and the double-step voltage inputs in time are prescribed as the Dirichlet boundary conditions of the electrostatic potential, $\phi_l = 0$mV, $\phi_r = \phi_r(t)$mV. The initial data are taken as a quasi-steady state solution after a long time simulation, sometimes called a 'prepotential' in the experimental literature, with $\phi_l = 0$mV, $\phi_r = -90$mV. The profiles of the initial data for the charge densities are presented in the right picture of Figure 2. To solve the MPNP-C system (3.6), (3.7), the edge averaged finite element method is employed [34]. The detailed algorithm for solving PNP type equations is presented in [2, 3].

The total current I and the individual currents I_i for the ith ion species are computed by

$$\vec{I} = \sum_{i=1}^{N} \vec{I}_i, \quad \vec{I}_i = z_i q \int \vec{J}_i \, d\vec{S} \approx z_i q S_{\text{eff}} \vec{\nu} \vec{J}_i$$

where S_{eff} is the effective cross sectional area of the channel, which is calculated as $S_{\text{eff}} = R_{ch}^2 \pi$ in the numerical computations [35], and $\vec{\nu}$ is the outer unit normal.

Note that all of the (ionic) currents will be calculated by subtracting the displacement current computed at the quasi-steady state with $\phi_r = -90$ mV. Also, all the results of currents presented in this section are obtained by taking an average inside the channel.

To understand the effect of the term (3.8), derived from the geometric constraint potential energy (3.3), we will first compare the difference of charge density profiles between the MPMP-C system and the MPNP in Figure 2. To decompose the effect of the energy (3.3) and compare it with the MPNP results in the MPNP-C system, we do numerical experiments on the MPNP system keeping the same

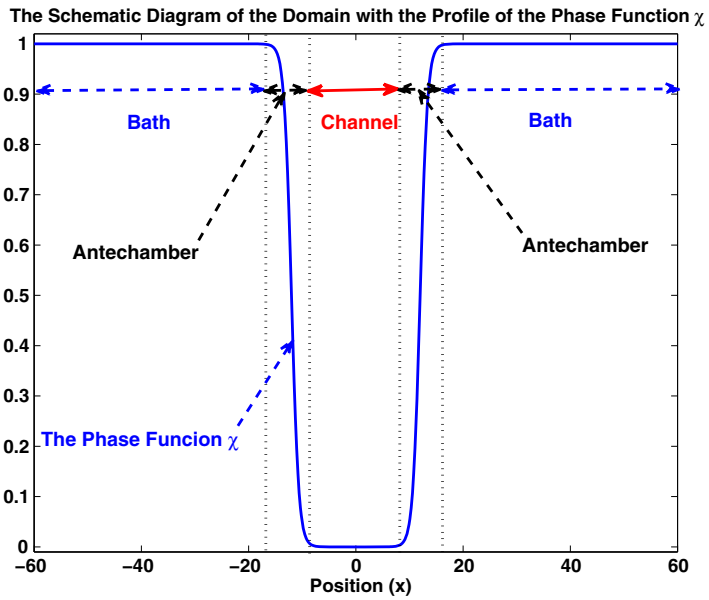

Figure 1. The schematic diagram of the domain with the profile of phase function χ in (3.2).

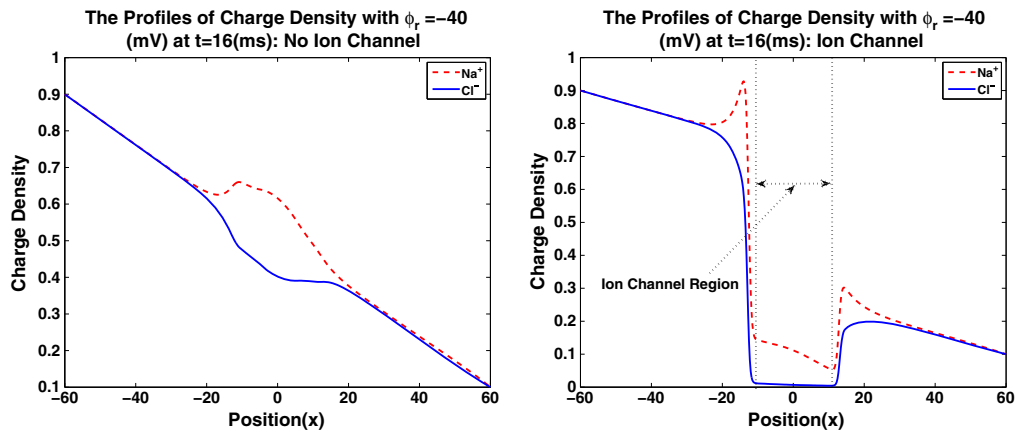

Figure 2. The profiles of charge densities without ion channel (left) and with ion channel (right) with $\phi_r = -40$ mV at $t = 16$ ms.

distributions of permanent charge and dielectric constant. The left picture is the charge density profile from the MPNP. Note the bumps in the center region. These are produced by the permanent charge and the dielectric constant difference between the channel and the bath. The charge density profiles produced by the channel potential energy of MPNP-C system are presented in the right picture of Figure 2. One can easily observe the influence of the channel potential energy that forms the ion channel at the center region. Also, the charge densities in the antechamber region have well-defined and simple profiles. Moreover, accumulation of charges inside and near the antechambers is distinctly observed and well captured. The diffuse interface method, with the phase function (3.2), allows the reliable calculation of the charge accumulation and profiles of charge. Previous calculations without the diffuse interface showed the existence of these phenomena but did not allow robust reliable calculation of their values and variation with conditions. These accumulations of charge have been studied extensively in the experimental literature and are called 'gating charge' or 'gating currents'.

In the channel potential function (3.3), the electric and mechanical properties of the channels are tied to the parameter values in the functionals. Here, we compare results for different parameters ρ_0 and A in Figure 3. First, we vary the permanent charge density ρ_0

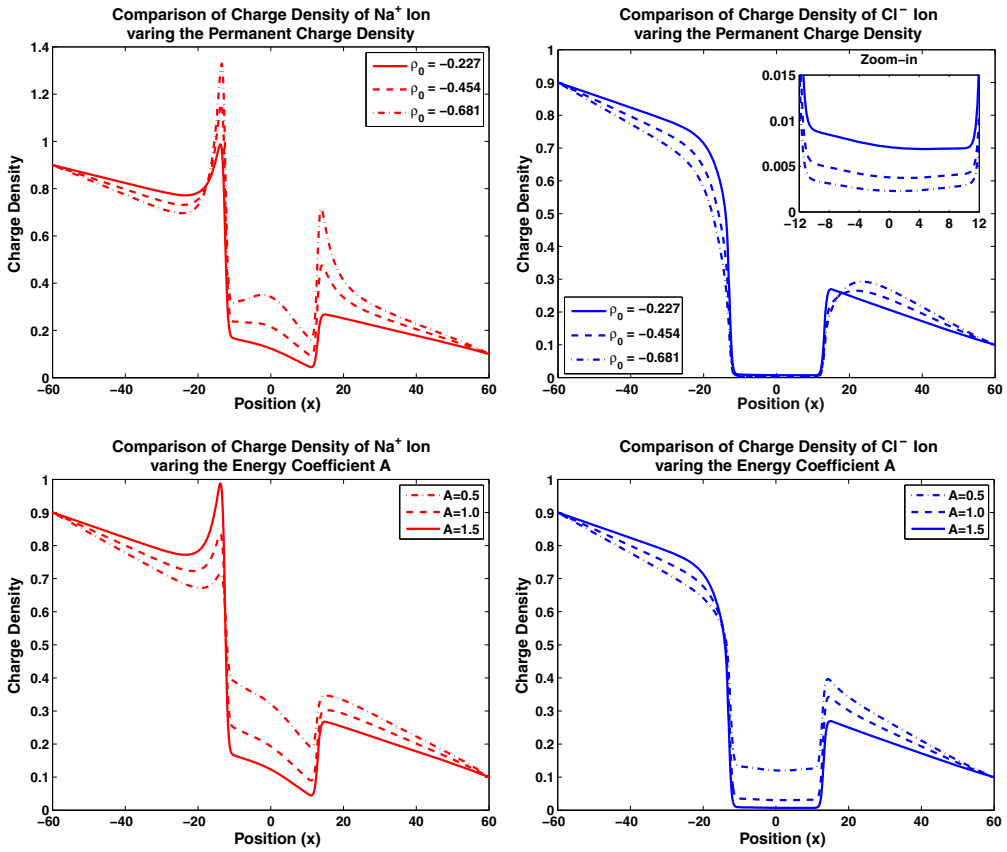

Figure 3. Comparisons of the charge densities for Na^+ (left), Cl^- (right) varying the permanent charge density ρ_0 (top) and the coefficient A in (3.3) (bottom).

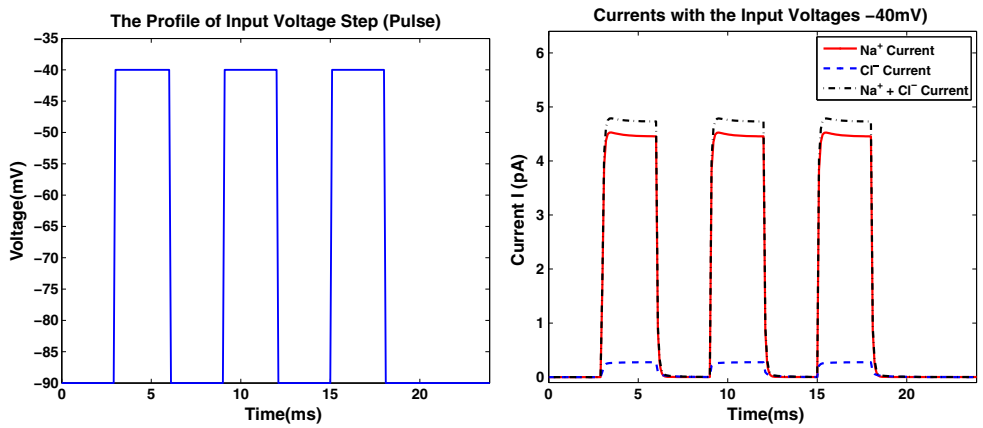

Figure 4. The single-step voltage input with −40 mV (left), and the currents of Na^+ (red solid), Cl^- (blue dash) and $Na^+ + Cl^-$ (black dash-dotted) (right). [The right picture is replaced].

with the same value of the coefficient $A = 1.5$ (the top panels in Figure 3). Next, we change the stiffness of the channel by varying the coefficient A with the same permanent charge $\rho_0 = -0.227$. (the bottom panels in Figure 3). In the top pictures, one can easily see that Na^+ ion is significantly squeezed into the ion channel when the strength of the permanent charge density increases from $|\rho_0| = 0.227$ to $|\rho_0| = 0.681$, whereas Cl^- flows out a little from the channel. When the coefficient A varies from 0.5 to 1.5, the results show that the larger value of A presses the charge densities down. These two experiments show the smoothness/stiffness of the channel, which is established by the channel potential designed by the diffusive interface method.

The first numerical experiment as a biophysical application of the MPNP-C system is the single step pulse with the input voltage -40 mV for the step. The input pulses of voltage and the output current are presented in Figure 4 as a function of time. The bump behavior of the currents at the beginning of the pulse is explained by the initial data obtained in a quasi-steady state solution and the steepness of the voltage input. According to the results in the right picture of Figure 4, a stabilization of the currents at the start-up for each step in the pulse is observed as the time goes on, 4.785 at time = 3.4 ms, 4.781 (pA) at time = 6.4 ms, and 4.781 (pA) at time = 9.4 ms in the total current.

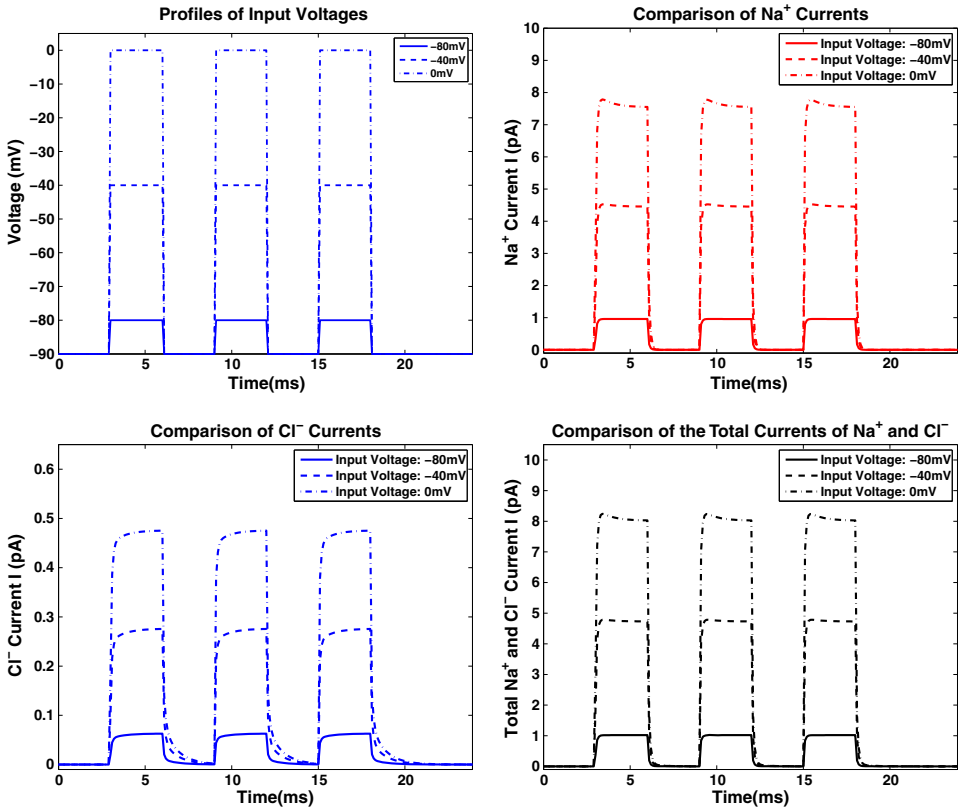

Figure 5. The single-step voltage inputs (top left), and the currents of Na^+ (top right), Cl^- (bottom left) and the total current of Na^+ and Cl^- (bottom right).

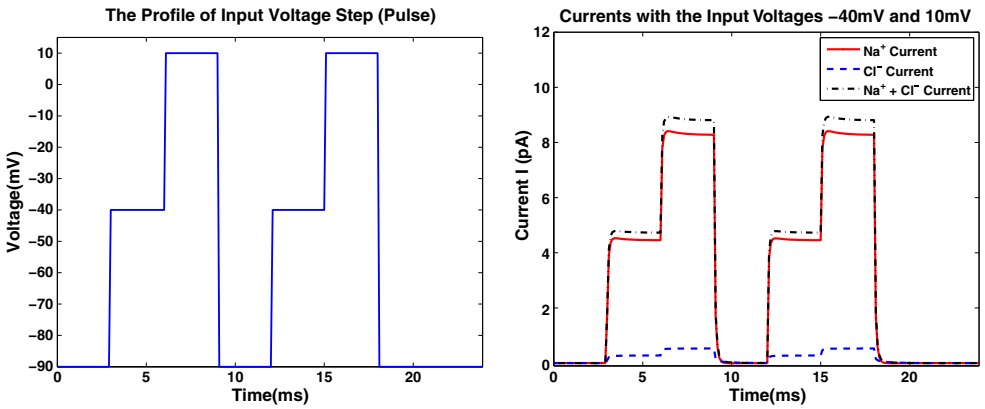

Figure 6. The double-step voltage input with -40 mV and 10 mV (left), and the currents of Na^+ (red solid), Cl^- (blue dash) and the total current of Na^+ and Cl^- (black dash-dotted) (right).

Next, we compare the current results with different input voltages, −80, −40, 0 mV. The comparisons are presented in Figure 5. As seen in the previous computations, the bump behavior of the currents and their stabilization are also observed as 8.243 (pA) at time = 3.4 ms, 8.236 (pA) at time = 6.4 ms, and 8.236 (pA) at time = 9.4 ms in the total current. When the input voltage is increased from −80 mV to 0 mV, the current is increases, but one can see that it is not linear to the input voltage. (See the current pictures in Figure 5.)

Remark 5.1
Note that the numerical computations of the mathematical model (3.6), (3.7) are performed in the situation of a permanently open ion channel. The opening and closing mechanism is not included in the model. All time dependence calculated here is a property of the physics of the open channel, and does not reflect the properties of an anatomically distinct gating structure [36].

The numerical computation of the pulse with the double-step input voltage is performed with $\phi_r = -40, 10$mV in 3 ms interval, and its numerical results are presented in Figure 6. In these results, we observe that the current increment from the first step to the second step is smaller than that from the initial to the first step. This nonlinear current behavior is consistent to the results in the comparison of the different voltage inputs of the single steps shown in Figure 5.

6. Conclusion

In this paper, we study the ion channel dynamics in the general framework of the energetic variational approach. This allows us to include different physics and constraints involved in the ion transport through proteins. We define a potential energy that maintains the local size of the ion channel. The diffusive interface method is used in the representation of the energy functional. The model allows the calculation of charge distributions that were previously difficult to evaluate because of the presence of different regions and interfaces. Numerical experiments for interesting channel dynamics were performed to verify the applicability of the model. These channel experiments also demonstrate the robustness and flexibility of the method.

Acknowledgements

The research of Chun Liu is partially supported by NSF grants DMS-0707594 and DMS-1109107. YunKyong Hyon is supported by KRCF Research Fellowship for Young Scientists and NIMS in Korea. Bob Eisenberg is supported by the Bard Endowed Chair of Rush University.

References

1. Eisenberg B, Hyon Y, Liu C. Energy variational analysis EnVarA of ions in water and channels: field theory for primitive models of complex ionic fluids. *Journal of Chemical Physics* 2010; **133**:104104-1–23.
2. Hyon Y, Eisenberg B, Liu C. A mathematical model for the hard sphere repulsion in ionic solutions. *Communications in Mathematical Sciences* 2011; **9**(2):459–475.
3. Hyon Y, Fonseca JE, Eisenberg B, Liu C. Energy variational approach to study charge inversion (layering) near charged walls. *DCDS-B* 2012; **17**(8):2725–2743.
4. Hyon Y, Kwak DY, Liu C. Energetic variational approach in complex fluids: maximum dissipation principle. *DCDS-A* 2010; **24**(4):1291–1304.
5. Ryham R. An energetic variational approach to mathematical modeling of charged fluids: charge phases, simulation and well posedness. *Thesis*, Pennsylvania State University, 2006.
6. Boda D, Nonner W, Valiskó M, Henderson D, Eisenberg B, Gillespie D. Steric selectivity in Na channels arising from protein polarization and mobile side chains. *Biophysical Journal* 2007; **93**:1960–1980.
7. Eisenberg RS. Computing the field in proteins and channels. *Journal of Membrane Biology* 1996; **150**:1–25.
8. Eisenberg B. Ionic channels in biological membranes: natural nanotubes. *Accounts of Chemical Research* 1998; **31**:117–123.
9. Eisenberg B. Crowded charges in ion channels. In *Advances in Chemical Physics*. John Wiley & Sons, Inc., 2011; 77–223. Available at: http:\arix.orgasarXiv1009.1786v1001 [Accessed on 9 September 2010].
10. Hille B. *Ion Channels of Excitable Membranes*, (3rd edn). Sinauer Associates, Inc.: Sunderland MA 01375-0407 USA, 2001.
11. Nonner W, Chen DP, Eisenberg B. Progress and prospects in permeation. *Journal of General Physiology* 1999; **113**:773–782.
12. Eisenberg B. Proteins, channels, and crowded ions. *Biophysical Chemistry* 2003; **100**:507–517.
13. Eisenberg B. Living transistors: a physicist's view of ion channels. version 2., 2008. Available from: http://arxiv.org/abs/q-bio/0506016v2 [Accessed 3 February 2008].
14. Eisenberg R, Chen D. Poisson-Nernst-Planck (PNP) theory of an open ionic channel. *Biophysical Journal* 1993; **64**:A22.
15. Nonner W, Catacuzzeno L, Eisenberg B. Binding and selectivity in L-type Ca channels: a mean spherical approximation. *Biophysical Journal* 2000; **79**:1976–1992.
16. Nonner W, Eisenberg B. Ion permeation and glutamate residues linked by Poisson-Nernst-Planck theory in L-type calcium channels. *Biophysical Journal* 1998; **75**:1287–1305.
17. Anderson DM, McFadden GB. Diffuse-interface methods in fluids mechanics. *Annual Review of Fluid Mechanics* 1998; **30**:139–165.
18. Cahn JW, Hilliard JE. Free energy of a nonuniform system. I. Interfacial free energy. *Journal of Chemical Physics* 1958; **28**:258–267.
19. Cahn JW, Hilliard JE. Free energy of a nonuniform system. III. Nucleation in a two-component incompressible fluid. *Journal of Chemical Physics* 1959; **31**:688–699.
20. Cahn JW, Allen SM. A microscopic theory for domain wall motion and its experimental verification in Fe-Al alloy domain growth kinetics. *Journal de Physique. Colloques* 1978:C7–C51.
21. Liu C, Shen J. A phase field model for the mixture of two incompressible fluids and its approximation by a Fourier-spectral method. *Physica D* 2003; **179**:211–228.

22. Yue P, Feng JJ, Liu C, Shen J. A diffuse-interface method of simulating two-phase flows of complex fluids. *Journal of Fluid Mechanics* 2004; **515**:293–317.
23. Bezanilla F, Rojas E, Taylor RE. Time course of the sodium influx in squid giant axon during a single voltage clamp pulse. *Journal of Physiology* 1970; **207**(1):151–164.
24. Bezanilla F, Armstrong CM. Kinetic properties and inactivation of the gating currents of sodium channels in squid axon. *Philosophical Transactions of the Royal Society B-Biological Sciences* 1975; **270**(908):449–458.
25. Hodgkin AL, Huxley AF. The dual effect of membrane potential on sodium conductance in the giant axon of Loligo. *Journal of Physiology* 1952; **116**(4):497–506.
26. Conley EC, Brammar WJ. *The Ion Channel Facts Book IV: Voltage Gated Channels*. Academic Press: New York, 1999.
27. Heras JA. A formal interpretation of the displacement current and the instantaneous formulation of Maxwell's equations. *American Journal of Physics* 2011; **79**:409–416.
28. Markowich PA. *The Stationary Semiconductor Device Equations*. Springer-Verlag: Vienna, 1986.
29. Selberherr S. *Analysis and Simulation of Semiconductor Devices*. Springer-Verlag: New York, 1984.
30. Eisenberg RS, Klosek MM, Schuss Z. Diffusion as a chemical reaction: stochastic trajectories between fixed concentrations. *Journal of Chemical Physics* 1995; **102**:1767–1780.
31. Jacoboni C, Lugli P. *The Monte Carlo Method for Semiconductor Device Simulation*. Springer-Verlag: New York, 1989.
32. Jackson JD. *Classical Electrodynamics*, (3rd edn). Wiley: New York, 1998.
33. Eisenberg B. Ions in fluctuating channels: Transistors alive. *Fluctuation and Noise Letters* 2012; **11**:1240001.
34. Xu J, Zikatanov L. A monotone finite element scheme for convection-diffusion equations. *Mathematics of Computation* 1999; **68**(228):1429–1446.
35. Luchinsky DG, Tindjong R, Kaufman I, McClintock PVE, Eisenberg RS. Self-consistent analytic solution for the current and the access resistance in open ion channels. *Physical Review E* 2009; **80**:021925-1–12.
36. Bezanilla F. Voltage sensor movements. *Journal of General Physiology* 2002; **120**(4):465–473.